Published in final edited form as:

Science. 2014 September 12; 345(6202): 1254009. doi:10.1126/science.1254009.

Innate lymphoid cells regulate intestinal epithelial cell glycosylation

Yoshiyuki Goto[1,2,3], **Takashi Obata**[1,3], **Jun Kunisawa**[1,4,5], **Shintaro Sato**[1,2], **Ivaylo I. Ivanov**[6], **Aayam Lamichhane**[1], **Natsumi Takeyama**[1,7], **Mariko Kamioka**[1], **Mitsuo Sakamoto**[3], **Takahiro Matsuki**[8], **Hiromi Setoyama**[8], **Akemi Imaoka**[8], **Satoshi Uematsu**[9,10], **Shizuo Akira**[11], **Steven E. Domino**[12], **Paulina Kulig**[13], **Burkhard Becher**[13], **Jean-Christophe Renauld**[14], **Chihiro Sasakawa**[7,15,16], **Yoshinori Umesaki**[8], **Yoshimi Benno**[17], and **Hiroshi Kiyono**[1,2,5]

[1]Division of Mucosal Immunology, Department of Microbiology and Immunology, The Institute of Medical Science, The University of Tokyo, Tokyo 108-8639, Japan [2]Core Research for Evolutional Science and Technology, Japan Science and Technology Agency, Saitama 332-0012, Japan [3]Microbe Division/Japan Collection of Microorganisms, RIKEN BioResource Center, Tsukuba 305-0074, Japan [4]Laboratory of Vaccine Materials, National Institute of Biomedical Innovation, Osaka 567-0085, Japan [5]Division of Mucosal Immunology, International Research and Development Center for Mucosal Vaccines, The Institute of Medical Science, The University of Tokyo, Tokyo 108-8639, Japan [6]Department of Microbiology and Immunology, Columbia University Medical Center, New York, NY 10032, USA [7]Nippon Institute for Biological Science, Tokyo 198-0024, Japan [8]Yakult Central Institute, Tokyo 186-8650, Japan [9]Division of Innate Immune Regulation, International Research and Development Center for Mucosal Vaccines, The Institute of Medical Science, The University of Tokyo, Tokyo 108-8639, Japan [10]Department of Mucosal Immunology, School of Medicine, Chiba University, 1-8-1 Inohana, Chuou-ku, Chiba, 260-8670, Japan [11]Laboratory of Host Defense, WPI Immunology Frontier Research Center, Osaka University, Osaka 565-0871, Japan [12]Department of Obstetrics and Gynecology, Cellular and Molecular Biology Program, University of Michigan Medical Center, Ann Arbor, MI 48109-5617, USA [13]Institute of Experimental Immunology, University of Zürich, Winterthurerstrasse 190, Zürich CH-8057, Switzerland [14]Ludwig Institute for Cancer Research and Université Catholique de Louvain, Brussels B-1200, Belgium [15]Division of Bacterial Infection, The Institute of Medical Science, The University of Tokyo, Tokyo 108-8639, Japan [16]Medical Mycology Research Center, Chiba University, Chiba 260-8673, Japan [17]Benno Laboratory, Innovation Center, RIKEN, Wako, Saitama 351-0198, Japan

Abstract

The authors declare no conflicts of interest.

SUPPLEMENTARY MATERIALS

www.sciencemag.org/content/345/6202/1254009/suppl/DC1

Figs. S1 to S11

Table S1

Fucosylation of intestinal epithelial cells, catalyzed by fucosyltransferase 2 (Fut2), is a major glycosylation mechanism of host–microbiota symbiosis. Commensal bacteria induce epithelial fucosylation, and epithelial fucose is used as a dietary carbohydrate by many of these bacteria. However, the molecular and cellular mechanisms that regulate the induction of epithelial fucosylation are unknown. Here, we show that type 3 innate lymphoid cells (ILC3) induced intestinal epithelial *Fut2* expression and fucosylation in mice. This induction required the cytokines interleukin-22 and lymphotoxin in a commensal bacteria–dependent and –independent manner, respectively. Disruption of intestinal fucosylation led to increased susceptibility to infection by *Salmonella typhimurium*. Our data reveal a role for ILC3 in shaping the gut microenvironment through the regulation of epithelial glycosylation.

In the gastrointestinal tract, bilateral regulation between the gut microbiota and the host creates a mutually beneficial environment. The intestinal epithelium is a physical barrier that separates the environments inside and outside the mucosal surface. Intestinal epithelial cells (ECs) are the first line of defense against foreign antigens, including those from commensal and pathogenic bacteria. ECs play key roles in initiating and maintaining an immunologically appropriate and balanced environment in reaction to constant foreign stimulation (1). Resident commensal bacteria support the development of this functional mucosal immune system, and in turn, mucosal immune cells control the homeostasis of the gut microbiota and protect against pathogenic bacterial infection through intestinal ECs. In particular, type 3 innate lymphoid cells (ILC3) produce interleukin-22 (IL-22), which not only regulates the homeostasis of the commensal microbiota but also protects against *Citrobacter rodentium* infection, presumably by inducing EC-derived antimicrobial molecules such as RegIIIγ (2–5).

Fucosylated carbohydrate moieties expressed on intestinal ECs are involved in the creation of an environmental niche for commensal bacteria in mice and humans (6–10). Fucosylated glycans are generated by the addition of an L-fucose residue via an α1-2 linkage to the terminal β-D-galactose residues of glycan in a process catalyzed by fucosyltransferase. Two fucosyltransferases, Fut1 and Fut2, mediate intestinal epithelial fucosylation, and each enzyme acts on a distinct subset of epithelial cells. Fut1 regulates fucosylation of Peyer's patch (PP) M cells, whereas Fut2 is a key enzyme regulating intestinal columnar epithelial fucosylation and the production of secretory fucosylated ABO(H) histo-blood group antigens (11). Defective Fut2 has been shown to result in susceptibility to *Candida albicans* infection in mice (12). In addition, inactivating polymorphisms of *FUT2* are associated with metabolic abnormalities and infectious and inflammatory diseases in humans (13–19).

The importance of epithelial fucose has been explored through studies of host–microbe interactions. Signals from commensal bacteria are required for epithelial fucosylation (6). Specific commensals, in particular *Bacteroides*, have been shown to induce epithelial fucosylation and are able to catabolize fucose for energy or incorporate it into bacterial cellular components—capsular polysaccharides—that give microbes a survival advantage in competitive environments (8, 9). Indeed, a lack of Fut2 alters the diversity and composition of the fecal microbiota in humans and mice (20, 21). Therefore, epithelial fucose functions as a mediator between the host and commensal microbiota. Although a previous report

proposed a model in which *Bacteroides*–EC interaction mediates epithelial fucosylation (7), the precise mechanisms by which Fut2 regulates fucosylation remain largely unknown.

Microbiota induces epithelial fucosylation

Epithelial fucosylation, a major glycosylation process, occurs in the small intestine (10, 11). To assess the inductive mechanism of intestinal epithelial fucosylation, we first investigated the localization of fucosylated ECs (F-ECs) along the length of the small intestine, divided equally into four parts from the duodenum (part 1) to the terminal ileum (part 4), in naïve mice (Fig. 1A). The frequency of F-ECs, detected with the α(1,2)-fucose–recognizing lectin *Ulex europaeus* agglutinin-1 (UEA-1), was low in the duodenum and jejunum (part 1 and a portion of part 2; <15% F-ECs) and gradually increased toward the ileum (part 4; 40 to 90% F-ECs) (Fig. 1, A to C). Consistent with epithelial fucosylation, epithelial Fut2 expression was also higher in the ileum (Fig. 1D). Because greater numbers of microorganisms are present in the distal ileum than in the duodenum (22), it may be possible that high numbers of ileal F-ECs are induced and maintained through microbial stimulation. To test this hypothesis, we examined the fucosylation status of ileal ECs (part 4) in mice treated with a mixture of antibiotics (AB), as well as in germ-free (GF) mice. The number of F-ECs was dramatically reduced in AB-treated and GF mice (Fig. 2A and fig. S1A). Furthermore, expression of epithelial *Fut2* was also reduced in AB-treated mice (Fig. 2B). Epithelial fucosylation was restored after cessation of AB treatment and in conventionalized GF mice (Fig. 2A and fig. S1A). In addition, fucosylation of goblet cells, but not Paneth cells, was lost in AB-treated and GF mice (Fig. 2C), indicating that commensal bacteria induce fucosylation of columnar epithelial cells and goblet cells, but not Paneth cells.

It has been shown that epithelial fucosylation can be induced by the mouse and human commensal *Bacteroides thetaiotaomicron* (6). However, on the basis of bacterial 16*S* ribosomal RNA (rRNA) gene clone library data obtained from isolated ileal mucus samples from naïve mice (Fig. 2D), we did not detect *B. thetaiotaomicron* in our colony, suggesting that other commensals can induce epithelial fucosylation. To identify which indigenous bacteria are responsible for the induction of F-ECs, we analyzed mucus-associated bacterial populations residing in the mouse duodenum (part 1) and ileum (part 4). In contrast to the predominance of *Lactobacillus* in the duodenum, segmented filamentous bacteria (SFB) predominated in the ileum (Fig. 2D); this is consistent with previous studies (23, 24). SFB are Gram-positive bacteria that preferentially colonize the epithelial surface of the terminal ileum, where they induce T helper 17 (T_H17) cells (25, 26). Similar to their effect on T_H17 cell–inducing microbiota (27), vancomycin, ampicillin, and to some extent metronidazole—but not neomycin—extinguished epithelial fucosylation (fig. S1, B and C). Furthermore, consistent with the emergence of SFB, epithelial fucosylation is initiated after weaning (6, 28). To investigate whether SFB have the potential to induce F-ECs, we examined mono-associated gnotobiotic mice and found that F-ECs were induced in SFB but not in *Lactobacillus murinus* mono-associated mice (Fig. 2E). Together, these results suggest that epithelial fucosylation in the terminal ileum is induced by commensal bacteria, including SFB, under physiological conditions.

ILC3 are required for epithelial fucosylation

We next investigated the cellular and molecular mechanisms of F-EC induction. Commensal bacteria, including SFB, induce the proliferation of intraepithelial lymphocytes and immunoglobulin A (IgA)–producing cells and the development of T_H17 cells; they also modulate the function of ILCs (3, 4, 25–27, 29). To assess whether epithelial fucosylation is induced directly by commensal bacteria or is mediated by mucosal immune cells, we first analyzed the epithelial fucose status of T cell–, B cell–, and Rag-deficient mice. The number of F-ECs was not decreased in T cell– or B cell–deficient mice (fig. S2), indicating that T cells and B cells are dispensable for the induction of epithelial fucosylation. Although SFB induce T_H17 cells (25, 26), T_H17 cells are not required for epithelial fucosylation because IL-6, a critical cytokine for T_H17 cell differentiation in the intestine (30), was also not necessary for the induction of F-ECs (fig. S3, A to C). We next analyzed RAR-related orphan receptor–γt (RORγt)–deficient mice, which lack the ILC3 subset, in addition to T_H17 cells (30, 31). RORγt-deficient mice exhibited a marked decrease in the number of F-ECs, accompanied by a decrease in *Fut2* expression in ileal ECs (Fig. 3, A to D). These findings suggest that ILC3 are critical inducers of F-ECs. This was further supported by our observation of few F-ECs in the ileum of Id2-deficient mice, which do not develop any of the ILC subsets (Fig. 3, E to G) (31, 32). Although both RORγt- and Id2-deficient mice lack PPs (33, 34), PPs are not necessary for epithelial fucosylation because PP-null mice, generated by treatment with monoclonal antibody (mAb) to IL-7R during fetal growth, had normal levels of F-ECs (fig. S4). ILC3 in the small intestine are aberrantly expanded in Rag-deficient mice (35), and elevated numbers of F-ECs were observed in these mice (Fig. 3, H and I), supporting the notion that F-ECs are induced by ILC3. Because ILC3 express higher levels of CD90, they can be depleted with a mAb to CD90 (36, 37). To identify whether ILC3 induce F-ECs, we treated wild-type and Rag-deficient mice with a mAb to CD90. *Fut2* expression and the number of F-ECs were markedly decreased after depletion of ILCs in both wild-type and Rag-deficient mice (Fig. 3, J to M, and fig. S5, A and B). Substantial numbers of SFB were still observed in RORγt-, Id2-, and $CD90^+$ ILC–depleted mice (fig. S6, A and B). Therefore, the defective epithelial fucosylation in these models was not attributable to the absence of F-EC–inducing commensals. Collectively, these results indicate that $CD90^+$ ILC3 are required for the induction and maintenance of F-ECs.

IL-22 produced by ILC3 mediates epithelial fucosylation

We next investigated how ILC3 induce epithelial fucosylation. ILC3 cells secrete IL-22, which stimulates the antimicrobial function and maintenance of intestinal ECs (3, 4, 36, 38). Indeed, the expression of *Il22* gene was much higher in ILC3 than in any other intestinal immune cell subset (fig. S7A). We therefore assessed whether commensal bacteria regulate ILC3 differentiation and cytokine expression. Although AB-treated or wild-type mice had similar numbers of $CD3^-$ $ROR\gamma t^+$ ILC3 (fig. S7, B and C), expression of lL-22 was significantly reduced in AB-treated mice but was restored after cessation of AB treatment (fig. S7D). To identify whether IL-22 is involved in the induction of F-ECs, we analyzed mice lacking IL-22 and found that they had reduced numbers of F-ECs; this was correlated with a decrease in epithelial *Fut2* expression (Fig. 4, A and B). We next examined whether IL-22 alone induced epithelial fucosylation. We used hydrodynamic delivery of an *Il22*-

encoding plasmid vector so as to ectopically overexpress IL-22 in AB-treated mice (fig. S8, A and B). In both AB-treated wild-type and *Rorc*$^{gfp/gfp}$ mice, F-ECs were induced in both the duodenum (part 1) and the ileum (part 4) in mice ectopically producing IL-22 but not in mice receiving control vector (Fig. 4, C and D, and fig. S8, C and D). This suggests that IL-22 is sufficient for epithelial fucosylation. Expression of *Fut2* was correlated with the presence of IL-22–induced F-ECs (Fig. 4E). To confirm whether IL-22 produced by ILC3 is necessary for epithelial fucosylation, Rag-deficient mice were treated with an antibody in order to neutralize IL-22. Epithelial *Fut2* expression and fucosylation were interrupted by the neutralization of IL-22 (Fig. 4, F to H). Microbial analyses of IL-22–deficient and antibody-to-IL-22–treated Rag-deficient mice revealed the presence of SFB (fig. S6, A and B). These findings demonstrate that ILC3-derived IL-22 induced by commensal bacteria mediates epithelial fucosylation. Furthermore, depletion of ILC3 by injecting antibody to CD90 into Rag-deficient mice resulted in marked reduction of IL-22 expression (Fig. 4I), supporting the notion that IL-22–mediated signals produced by ILC3 are a key part of the EC fucosylation cascade. IL-22R is composed of two subunits, IL-22R1 and IL-10Rβ (39). Whereas IL-10Rβ was ubiquitously expressed, expression of IL-22R1 was specifically detected in intestinal ECs and was not reduced, even after the depletion of commensal bacteria (fig. S9, A and B). Taken together, our findings indicate that commensal bacteria provide signals that prompt ILC3 to produce IL-22, which leads to the induction of Fut2 by IL-22R–positive intestinal ECs.

LTα expressed by ILC3 induces epithelial fucosylation

ILC3 support the development and maintenance of secondary lymphoid tissues through the expression of lymphotoxins (LTs)—especially LTα1β2 (40). The expression of *Lta* and *Ltb* genes was higher in ILC3 than in any other intestinal immune cell subset (fig. S10A). In contrast to IL-22, which was induced by commensal bacteria, *Lta* and *Ltb* gene expression in ILC3 was not affected by commensal flora because the AB treatment did not alter the gene expression (fig. S10B). However, intestinal epithelial fucosylation and *Fut2* expression were severely impaired in *Lta*$^{-/-}$ mice (Fig. 5, A to C). *Lta*$^{-/-}$ mice possess congenital defects in secondary lymphoid organs (41). To elucidate the contribution of LTα to epithelial fucosylation in adult mice that have established secondary lymphoid organs, wild-type mice were treated with LTβR-Ig, which blocks LTα1β2 signaling. Epithelial fucosylation was attenuated by treatment with LTβR-Ig (Fig. 5, D to E), implying that a continuous LT signal is required for epithelial fucosylation. To investigate whether LTα in ILC3 is crucial for the induction of F-ECs, we constructed mixed bone marrow (BM) chimeric mice by transferring BM cells taken from LTα-deficient or -sufficient mice and mixed with BM cells from RORγt-deficient mice into lethally irradiated recipients. F-ECs and *Fut2* expression were diminished in recipient mice reconstituted with BM cells containing LTα-deficient RORγt^{+} ILC3, whereas substantial numbers of F-ECs, and *Fut2* expression, were induced in recipient mice reconstituted with BM cells containing LTα-sufficient RORγt^{+} ILC3, indicating the importance of LTα expressed by ILC3 in the induction of F-ECs (Fig. 5, F to H). When the microbiota of LTα-deficient mice or of mixed BM chimeras containing LTα-deficient ILC3 were examined, substantial numbers of SFB were observed (fig. S6, A and

B). From these results, we concluded that induction and maintenance of F-ECs were also regulated by ILC3-derived LT in a commensal flora–independent manner.

Epithelial fucosylation protects against infection by *Salmonella typhimurium*

We next investigated the physiological role of epithelial fucosylation. With exception of Paneth cells, the *Fut2* expression and ileal epithelial fucosylation observed in wild-type mice were abolished in *Fut2*$^{-/-}$ mice (fig. S11, A to E). We did not detect any overt changes in mucosal leukocyte populations or in IL-22 or LT expression in ILC3 in these mice (fig. S11F and table S1). Epithelial fucosylation provides an environmental platform for colonization by *Bacteroides* species (6–9); however, it is unknown whether epithelial fucosylation affects colonization and subsequent infection by pathogenic bacteria. To assess the effects of intestinal fucosylation on pathogenic bacterial infection, we first infected GF mice with the enteropathogenic bacterium *Salmonella typhimurium*, which has the potential to attach to fucose-containing carbohydrate molecules (42). After infection with *S. typhimurium*, ECs from both part 1 (duodenum) and part 4 (ileum) of the mouse intestine were fucosylated, and this was correlated with Fut2 expression (Fig. 6, A and B). Previous reports have shown that expression of IL-22 in ILCs is much higher in mice infected with *S. typhimurium* (43, 44). Therefore, *S. typhimurium*–induced epithelial fucosylation may be mediated by ILC3. Indeed, epithelial fucosylation was not induced in RORγt-deficient mice after *S. typhimurium* infection (Fig. 6C). To investigate whether epithelial fucosylation has a role in regulating pathogenic bacterial infection, we infected wild-type or *Fut2*$^{-/-}$ mice with *S. typhimurium* and examined disease progression. Compared with wild-type mice, *Fut2*$^{-/-}$ mice were more susceptible to *Salmonella* infection accompanied with the observation of severe inflamed cecum (Fig. 6D). Consistent with the inflammatory status of diseased mice, the numbers of infiltrating leukocytes in cecum were higher in *Fut2*$^{-/-}$ mice than in wild-type mice (Fig. 6E). Although *S. typhimurium* titers in cecal contents were comparable between wild-type and *Fut2*$^{-/-}$ mice, increased numbers of *S. typhimurium* infiltrated the cecal tissue of *Fut2*$^{-/-}$ mice (Fig. 6F). These results suggest that epithelial fucosylation is dispensable for luminal colonization by *S. typhimurium* but inhibits bacterial invasion of intestinal tissues. Collectively, these results indicate that epithelial fucosylation, regulated by *Fut2*, has a protective role against infection by pathogenic bacteria.

Discussion

The results of recent genome-wide association studies imply that FUT2 nonsense polymorphisms affect the incidence of various metabolic and inflammatory diseases, including chronic intestinal inflammation such as Crohn's disease and infections with pathogenic microorganisms, especially Norwalk virus and rotavirus in humans (13–19). Understanding the mechanisms of regulation of Fut2 gene expression and fucosylation, one of the major glycosylation events in intestinal ECs, is therefore of great interest. Previously, it was thought that epithelial fucosylation is initiated by direct interaction between commensals and ECs (7). Indeed, several reports have shown that epithelial fucosylation is actively induced and used by *Bacteroides* (8, 9). Here, we unexpectedly found that

microbiota–epithelia cross-talk is insufficient to induce epithelial fucosylation, and rather, CD90$^+$ RORγt$^+$ ILC3 are necessary for induction of epithelial *Fut2* expression and consequent fucosylation. ILC3 located in the intestinal lamina propria express high levels of IL-22 in a commensal bacteria–dependent manner (Fig. 4I and fig. S7, A and D). This IL-22 then presumably binds to IL-22R expressed by intestinal ECs, leading to the induction of Fut2 and initiation of the EC fucosylation process (Fig. 7). In contrast to the expression of IL-22, ILC3 express LT in a commensal bacteria–independent manner. Spontaneous expression of LT on ILC3 also contributes to the induction of epithelial fucosylation. To explain the mechanism underlying induction of epithelial fucosylation, we propose that epithelial fucosylation is regulated by a two-phase system orchestrated by ILC3 through the microbiota-independent production of LT and the induction of IL-22 by commensal bacteria (Fig. 7). Although other types of stimulation may also affect epithelial fucosylation, our findings reveal a critical role for ILC3.

Our results demonstrated that IL-22 produced by ILC3 is necessary and sufficient for induction of epithelial fucosylation when ILC3 are appropriately stimulated by commensal microbiota (Fig. 4, A to E). In addition to IL-22–mediated epithelial fucosylation, our results also show that the level of epithelial fucosylation is markedly reduced under LTα-deficient conditions (Fig. 5, A to C). Our findings suggest two possibilities for the IL-22/LT–mediated regulation of epithelial fucosylation. The first is that Fut2 expression and subsequent epithelial fucosylation are induced when the intensity of synergistic or additive signals from IL-22 and LT is above the threshold for activation of Fut2. For example, LT produced by ILC3 provides the baseline signal for the minimum expression of Fut2, whereas commensal-mediated IL-22 produced by ILC3 drives the maximum expression of Fut2 for the induction of epithelial fucosylation. The second possibility is that LT directly or indirectly regulates the expression of IL-22R by ECs, and vice versa, and/or the expression of IL-22. Indeed, a previous report has shown that LT produced by ILC3 regulates the expression of IL-23 by intestinal dendritic cells, as well as the subsequent production of IL-22 by ILC3 after infection with *C. rodentium* (45). How ILC3-derived IL-22 and LT regulate epithelial Fut2 expression remains to be further elucidated.

Our findings provide further evidence of the critical roles of commensal microbiota, epithelial cells, and innate immune cells (such as ILC3) in the creation of a protective platform against infection by pathogenic bacteria (Fig. 7). Ablation of epithelial fucose allowed severe infection by the pathogenic bacteria *S. typhimurium* (Fig. 6, D to F). Although the detailed mechanisms of why *Fut2*$^{-/-}$ mice are susceptible to *Salmonella* infection remain unknown, one possibility is that fucosylated mucin produced by goblet cells blocks the attachment of *S. typhimurium* to the epithelium. Commensal microbes continuously stimulated goblet cells to release fucosylated mucin into the intestinal lumen (Fig. 2C). Indeed, in a previous in vitro study, H-type 2 antigens, which are synthesized by Fut2 in intestinal ECs, prevented the binding of *S. typhimurium* to fucosylated epithelia; this supports our present findings (42). Our findings suggest a protective role for ILC3-mediated mucus-associated fucosylated glycan against infection by pathogenic bacteria.

ILC3 play critical roles in regulation of immune responses during mucosal infection, especially by producing IL-22, which promotes subsequent expression of the antimicrobial

molecule RegIIIγ by ECs (4, 36, 45). In addition to this, our results describe a previously unknown biological role for ILC3 in the induction and maintenance of intestinal epithelial glycosylation, which leads to the creation of an antipathogenic bacterial platform in the intestine (Fig. 7). Furthermore, epithelial fucosylation contributes to the creation of a cohabitation niche for the establishment of normal commensal microbiota (20, 21). Thus, ILC3-mediated control of epithelial-surface glycosylation might represent a general strategy for regulating the gut microenvironment. Targeted modification of these mechanisms has the potential to provide novel approaches for the control of intestinal infection and inflammation.

Materials and Methods

Mice

C57BL/6 and BALB/c mice were purchased from CLEA Japan (Tokyo, Japan). *Fut2*$^{-/-}$ and *Il22*$^{-/-}$ mice (C57BL/6 background) were generated as described previously, and *Id2*$^{-/-}$ mice were kindly provided by Y. Yokota (33, 46, 47). *Fut2*$^{-/-}$ mice were crossed onto the BALB/c background for six generations. *Rag2*$^{-/-}$ mice were kindly provided by F. Alt. *Rag1*$^{-/-}$; *Rorc*$^{gfp/gfp}$, *Il6*$^{-/-}$, *Ltα*$^{-/-}$, *Tcrβ*$^{-/-}$*δ*$^{-/-}$, and *Igh6*$^{-/-}$ mice were purchased from The Jackson Laboratory. Antibiotic-treated mice were fed a cocktail of broad-spectrum antibiotics—namely, ampicillin (1 g/L; Sigma, Bandai, Japan), vancomycin (500 mg/L; Shionogi, Osaka, Japan), neomycin (1 g/L; Sigma), and metronidazole (1 g/L; Sigma)—or were given these antibiotics in their drinking water, for 4 weeks as previously described (48). These mice were maintained in the experimental animal facility at the University of Tokyo. GF and SFB or *L. murinus* gnotobiotic mice (BALB/c) were maintained in the GF animal facility at the Yakult Central Institute and at the University of Tokyo. In all experiments, littermates were used at 6 to 10 weeks of age.

Isolation of bacterial DNA

The isolation protocol for bacterial DNA was adapted from a previously described method (49), with some modifications. Bacterial samples in the duodenum and ileum were obtained from mice aged 8 weeks. After removal of PPs and intestinal contents, the intestinal tissues were washed three times with phosphate-buffered saline (PBS) for 10 s each time so as to collect bacteria embedded within the intestinal mucus for analysis of microbial composition. These bacteria-containing solutions were centrifuged, and the pellets were suspended in 500 μL of TE buffer (10 mM Tris-HCl, 1 mM EDTA; pH 8.0). Glass beads, Tris-phenol buffer, and 10% sodium dodecyl sulfate (SDS) were added to the bacterial suspensions, and the mixtures were vortexed vigorously for 10 s by using a FastPrep FP100 A (BIO 101). After incubation at 65°C for 10 min, the solutions were vortexed and incubated again at 65°C for 10 min. Bacterial DNA was then precipitated in isopropanol, pelleted by centrifugation, washed in 70% ethanol, and resuspended in TE buffer. Extracted bacterial DNA was subjected to 16*S* rRNA gene clone library (50).

16S rRNA gene clone library analyses

For 16*S* rRNA gene clone library analyses, bacterial 16*S* rRNA gene sequences were amplified by means of polymerase chain reaction (PCR) with the 27F (5′-

AGAGTTTGATCCTGGCTCAG-3′) and 1492R (5′-GGTTACCTTGTTACGACTT-3′) primers. Amplified 16*S* rDNA was ligated into the pCR4.0 TOPO vector (Invitrogen, Carlsbad, CA), and the products of these ligation reactions were then transformed into DH-5α–competent cells (TOYOBO, Osaka, Japan). Inserts were amplified and sequenced on an ABI PRISM 3100 Genetic Analyzer (Applied Biosystems, Foster City, CA). The 27F and 520R (5′-ACCGCGGCTGCTGGC-3′) primers and a BigDye Terminator cycle sequencing kit (Applied Biosystems) were used for sequencing. Bacterial sequences were identified by means of Basic Local Alignment Search Tool (BLAST) and Ribosomal Database Project searches (50).

Immunohistochemistry

Immunohistochemical analyses were performed as previously described, with some modifications (51). For whole-mount immunofluorescence staining, the mucus layer was removed by flushing the small intestine with PBS; then, the appropriate parts of the small intestine were fixed with 4% paraformaldehyde for 3 hours. After being washing with PBS, whole-mount tissues were stained for at least 3 hours at 4°C with 20 μg/mL UEA-1 conjugated to tetramethylrhod-amine B isothiocyanate (UEA-1-TRITC; Vector Laboratories, Burlingame, CA) and 10 μg/mL wheat germ agglutinin (WGA) conjugated to Alexa Fluor 633 (Invitrogen). For whole-mount fluorescence in situ hybridization analysis, we modified the protocol previously described (52). After fixation with 4% paraformaldehyde, intestinal tissues were washed with 1 mL PBS and 100 μL hybridization buffer (0.9 M NaCl, 20 mM Tris-HCl, 0.1% SDS) containing 2 μg EUB338 probe (5′-GCTGCCTCCCGTAGGAGT-3′) conjugated to Alexa Fluor 488 (Invitrogen). After overnight incubation at 42°C, the tissues were washed with 1 mL PBS and stained for 3 hours with 10 μg/mL WGA conjugated to Alexa Fluor 633 in PBS. After being washed with PBS, all tissues were analyzed under a confocal laser-scanning microscope (TCS SP2; Leica Microsystems, Wetzlar, Germany).

Cell preparations

A standard protocol was used to prepare intestinal ECs (53). Tissues of the small intestine were extensively rinsed with PBS after removal of PPs. After the intestinal contents had been removed, the samples were opened longitudinally and cut into 1-cm pieces. These tissue pieces were mildly shaken in 1 mM EDTA/PBS for 10 min at 37°C. After passage through a 40-μm mesh filter, intestinal ECs were resuspended in minimum essential medium containing 20% fetal calf serum (FCS). Lamina propria (LP) cells were collected as previously described (54), with some modifications. Briefly, isolated small intestine was shaken for 40 min at 37°C in RPMI 1640 containing 10% FCS and 1 mM EDTA. Cell suspensions, including intestinal ECs and intraepithelial lymphocytes, were discarded, and the remaining tissues were further digested with continuous stirring for 60 min at 37°C with 2 mg/mL collagenase (Wako) in RPMI 1640 containing 10% FCS. After passage through a 190-μm mesh, the cell suspensions were subjected to Percoll (GE Healthcare) density gradients of 40 and 75%, and the interface between the layers was collected to retrieve LP cells. Stromal cells were identified as $CD45^-$ $Viaprobe^-$ cells. For fluorescence-activated cell-sorting (FACS) analysis of ILCs, isolated LP cells were further purified by magnetic-

activated cell sorting so as to eliminate $CD11b^+$, $CD11c^+$, and $CD19^+$ cells. $CD11b^-CD11c^-$ $CD19^-$ $Viaprobe^-$ $CD45^+$ LP cells were used to detect ILCs.

Antibodies and flow cytometry

For flow cytometric analysis, isolated intestinal ECs were stained with UEA-1-TRITC, anti-CD45–Pacific blue (PB; Biolegend, San Diego, CA), and Viaprobe (BD Biosciences, East Rutherford, NJ). $Viaprobe^-$ $CD45^-$ $UEA\text{-}1^+$ cells were identified as F-ECs. After blocking with anti-CD16/32 (FcγRII/III) (BD Biosciences), the following antibodies were used to stain spleen and LP cells: anti-CD45–PB (Biolegend), anti-CD11b–phycoerythrin (PE), anti-Foxp3-fluorescein isothiocyanate (FITC) (eBioscience, San Diego, CA), anti-CD11c–allophycocyanin (APC), anti-CD11b–FITC, anti-Gr-1-Alexa647, anti-CD3-APC, anti-B220-PE, anti-B220-APC, anti-IgA-FITC, anti-CD4-eFluor450, anti-CD90.2–FITC, anti-IL-17-PE, and anti-IFNγ-FITC (all from BD Biosciences), and Viaprobe. $CD11b^-$ $CD11c^-$ $CD19^-$ LP cells were purified by using anti-CD11b, anti-CD11c, and anti-CD19 MicroBeads (Miltenyi Biotec, Bergisch Gladbach, Germany). The results were obtained by using a FACSAria cell sorter (BD Biosciences) with FlowJo software (TreeStar, Ashland, Oregon).

Intracellular staining of Foxp3 and cytokines

Isolated LP cells were incubated for 4 hours at 37°C with 50 ng/mL phorbol myristate acetate (Sigma), 500 ng/mL ionomycin (Sigma), and GolgiPlug (BD Bioscience) in RPMI 1640 containing 10% FCS and penicillin and streptomycin. After incubation, cells were stained with antibodies against surface antigens for 30 min at 4°C. The cells were fixed and permeabilized with Cytofix/Cytoperm solution (BD Bioscience), and cytokines were stained with the fluorescence-conjugated cytokine antibodies. A Foxp3 staining buffer set (eBioscience) was used for intracellular staining of Foxp3.

Depletion of $CD90^+$ ILCs

Depletion of $CD90^+$ ILCs was performed as previously described, with some modifications (36). Two hundred and fifty micrograms of a mAb to CD90.2 or an isotype control rat IgG2b (BioXCell, West Lebanon, NH) was given by means of intra-peritoneal injection a total of three times at 3-day intervals. Intestinal ECs and LP cells were collected 2 days after the final injection.

Hydrodynamic IL-22 gene delivery system

pLIVE control plasmid (Takara Bio, Shiga, Japan) or IL-22–expressing pLIVE vector (pLIVE-*mIl22*) was introduced into 8-week-old antibiotic-treated C57BL/6 or $Rorc^{gfp/gfp}$ mice. Ten micrograms per mouse of plasmid diluted in ~1.5 mL TransIT-EE Hydrodynamic Delivery Solution (Mirus Bio, Madison, WI) was injected via the tail vein within 7 to 10 s. To assess IL-22 expression, serum IL-22 was quantified by means of an enzyme-linked immunosorbent assay (R&D Systems, Minneapolis, MN).

Generation of PP-null mice

mAb to IL-7R (A7R34) was kindly provided by S. Nishikawa. PP-null mice were generated by injecting 600 μg of mAb to IL-7R into pregnant mice on embryonic day 14 (55).

In vivo treatment with LTβR-Ig and antibody to IL-22

Neutralization antibody to IL-22 was purchased from eBioscience. Eight-week-old Rag-deficient mice were injected intraperitoneally with antibody to IL-22 a total of five times at 3-day intervals (on days 0, 3, 6, 9, and 12). Plasmid pMKIT-expressing LTβR-Ig and LTβR-Ig treatment was performed as described previously (56). Four-week-old C57BL/6 mice were injected intraperitoneally once a week for 3 weeks (on days 0, 7, 14, and 21) with LTβR-Ig fusion protein or control human IgG1 at a dose of 50 μg per mouse. Intestinal ECs were analyzed 3 days after the indicated injection time points.

Adoptive transfer of mixed BM

For mixed BM transfer experiments, *Rorc*$^{gfp/gfp}$ mice were irradiated with two doses of 550 rad each, 3 hours apart. BM cells (1×10^7) from *Rorc*$^{gfp/gfp}$ mice was mixed with BM cells (1×10^7) from C57BL/6 or *Lt*$\alpha^{-/-}$ mice and intravenously injected into irradiated recipient mice. BM chimeric mice were used for experiments 8 weeks after the BM transfer.

Isolation of RNA and real-time reverse transcriptase PCR analysis

Intestinal ECs and subsets of LP cells were sorted with a FACSAria cell sorter (BD Biosciences). The sorted cells were lysed in TRIzol reagent (Invitrogen), and total RNA was extracted in accordance with the manufacturer's instructions. RNA was reverse-transcribed by using a SuperScript VILO cDNA Synthesis Kit (Invitrogen). The cDNA was subjected to real-time reverse transcriptase–PCR (rRT-PCR) by using Roche (Basel, Switzerland) universal probe/primer sets specific for *Lt*α (primer F: 5′-tccctcagaagcacttgacc-3′, R: 5′-gagttctgcttgctggggta-3′, probe No. 62), *Lt*β (primer F: 5′-cctggtgaccctgttgttg-3′, R: 5′-tgctcctgagccaatgatct-3′, probe No. 76), *Il22* (primer F: 5′-tttcctgaccaaactcagca-3′, R: 5′-tctggatgttctggtcgtca-3′, probe No. 17), *Il22r1* (primer F: 5′;-tgctctgttatctgggctacaa-3′, R: 5′-tcaggacacgttggacgtt-3′, probe No. 9), *Il10r*β (primer F: 5′-attcggagtgggtcaatgtc-3′, R: 5′-gcatctcaggaggtccaatg-3′, probe No. 29), *Fut2* (primer F: 5′-tgtgacttccaccatcatcc-3′, R: 5′-tctgacagggtttggagctt-3′, probe No. 67), and *Gapdh* (primer F: 5′-tgtccgtcgtggatctgac-3′, R: 5′-cctgcttcaccaccttcttg-3′, probe No. 80). RT-PCR analysis was performed with a Lightcycler II instrument (Roche Diagnostics) to measure the expression levels of specific genes.

Infection with S. typhimurium

Streptomycin-resistant wild-type *S. typhimurium* was isolated from *S. typhimurium* strain ATCC 14028. *Fut2*$^{-/-}$ (BALB/c background) and control littermate mice pretreated with 20 mg of streptomycin 24 hours before infection were given 1×10^8 colony-forming units of the isolated *S. typhimurium* via oral gavage. After 24 hours, the mice were dissected, and the cecal contents were collected. Isolated cecum was treated with PBS containing 0.1 mg mL^{-1} gentamicin at 4°C for 30 min so as to kill bacteria on the tissue surface. The cecum was then homogenized and serial dilutions plated in order to determine the number of *S. typhimurium*. Sections of proximal colon were prepared 48 hours after infection. Infiltration of inflammatory cells was confirmed with hematoxylin and eosin staining.

Statistical analysis

Statistical analysis was performed with an unpaired, two-tailed Student's *t*-test. *P* values <0.05 were considered statistically significant.

Supplementary Material

Refer to Web version on PubMed Central for supplementary material.

Acknowledgments

We thank M. Shimaoka, G. Eberl, M. Pasparakis, K. Honda, C. A. Hunter, C. O. Elson, and J. R. Mora for their critical and helpful comments and advice on this research. Y. Yokota and M. Yamamoto kindly provided Id2-deficient mice and LTβR-Ig, respectively. R. Curtis III and H. Matsui kindly provided several strains of *Salmonella typhimurium*. We thank Y. Akiyama for her technical support with the *S. typhimurium* infection model. S. Tanaka gave us helpful technical suggestions for performing flow cytometric analysis. The data presented in this paper are tabulated in the main paper and in the supplementary materials. Sequences of the bacterial 16*S* rRNA genes obtained from duodenal and ileal mucus bacteria have been deposited in the International Nucleotide Sequence Database (accession nos. AB470733 to AB470815). This work was supported by grants from the following sources: the Core Research for Evolutional Science and Technology Program of the Japan Science and Technology Agency (to H.K.); a Grant-in-Aid for Scientific Research on Priority Areas, Scientific Research (S) (to H.K.); Specially Promoted Research (230000-12 to C.S.); Scientific Research (B) (to J.K.); for the Leading-edge Research Infrastructure Program and the Young Researcher Overseas Visits Program for Vitalizing Brain Circulation (to Y.G., J.K., and H.K.); for the Leading-edge Research Infrastructure Program (to J.K. and H.K.) from the Ministry of Education, Culture, Sports, Science and Technology of Japan; the Global Center of Excellence (COE) Program "Center of Education and Research for Advanced Genome-based Medicine" (to H.K.); the Ministry of Health, Labor and Welfare of Japan (to J.K. and H.K.); the Science and Technology Research Promotion Program for Agriculture, Forestry, Fisheries and Food Industry (to J.K.); Mochida Memorial Foundation for Medical and Pharmaceutical Research (to J.K.); the National Institutes of Health (1R01DK098378 to I.I.); and by the Crohn's and Colitis Foundation of America (SRA#259540 to I.I.).

REFERENCES AND NOTES

1. Goto Y, Ivanov II. Intestinal epithelial cells as mediators of the commensal-host immune crosstalk. Immunol Cell Biol. 2013; 91:204–214.10.1038/icb.2012.80 [PubMed: 23318659]
2. Qiu J, et al. Group 3 innate lymphoid cells inhibit T-cell-mediated intestinal inflammation through aryl hydrocarbon receptor signaling and regulation of microflora. Immunity. 2013; 39:386–399.10.1016/j.immuni.2013.08.002 [PubMed: 23954130]
3. Sanos SL, et al. RORgammat and commensal microflora are required for the differentiation of mucosal interleukin 22-producing NKp46$^+$ cells. Nat Immunol. 2009; 10:83–91.10.1038/ni.1684 [PubMed: 19029903]
4. Satoh-Takayama N, et al. Microbial flora drives interleukin 22 production in intestinal NKp46$^+$ cells that provide innate mucosal immune defense. Immunity. 2008; 29:958–970.10.1016/j.immuni.2008.11.001 [PubMed: 19084435]
5. Vaishnava S, et al. The antibacterial lectin RegIIIγ promotes the spatial segregation of microbiota and host in the intestine. Science. 2011; 334:255–258.10.1126/science.1209791 [PubMed: 21998396]
6. Bry L, Falk PG, Midtvedt T, Gordon JI. A model of host-microbial interactions in an open mammalian ecosystem. Science. 1996; 273:1380–1383.10.1126/science.273.5280.1380 [PubMed: 8703071]
7. Comstock LE, Kasper DL. Bacterial glycans: Key mediators of diverse host immune responses. Cell. 2006; 126:847–850.10.1016/j.cell.2006.08.021 [PubMed: 16959564]
8. Coyne MJ, Reinap B, Lee MM, Comstock LE. Human symbionts use a host-like pathway for surface fucosylation. Science. 2005; 307:1778–1781.10.1126/science.1106469 [PubMed: 15774760]

9. Hooper LV, Xu J, Falk PG, Midtvedt T, Gordon JI. A molecular sensor that allows a gut commensal to control its nutrient foundation in a competitive ecosystem. Proc Natl Acad Sci USA. 1999; 96:9833–9838.10.1073/pnas.96.17.9833 [PubMed: 10449780]
10. Goto Y, Kiyono H. Epithelial barrier: An interface for the cross-communication between gut flora and immune system. Immunol Rev. 2012; 245:147–163.10.1111/j.1600-065X.2011.01078.x [PubMed: 22168418]
11. Terahara K, et al. Distinct fucosylation of M cells and epithelial cells by Fut1 and Fut2, respectively, in response to intestinal environmental stress. Biochem Biophys Res Commun. 2011; 404:822–828.10.1016/j.bbrc.2010.12.067 [PubMed: 21172308]
12. Hurd EA, Domino SE. Increased susceptibility of secretor factor gene Fut2-null mice to experimental vaginal candidiasis. Infect Immun. 2004; 72:4279–4281.10.1128/IAI.72.7.4279-4281.2004 [PubMed: 15213174]
13. Franke A, et al. Genome-wide meta-analysis increases to 71 the number of confirmed Crohn's disease susceptibility loci. Nat Genet. 2010; 42:1118–1125.10.1038/ng.717 [PubMed: 21102463]
14. Hazra A, et al. Common variants of FUT2 are associated with plasma vitamin B12 levels. Nat Genet. 2008; 40:1160–1162.10.1038/ng.210 [PubMed: 18776911]
15. Lindesmith L, et al. Human susceptibility and resistance to Norwalk virus infection. Nat Med. 2003; 9:548–553.10.1038/nm860 [PubMed: 12692541]
16. McGovern DP, et al. International IBD Genetics Consortium. Fucosyltransferase 2 (FUT2) non-secretor status is associated with Crohn's disease. Hum Mol Genet. 2010; 19:3468–3476.10.1093/hmg/ddq248 [PubMed: 20570966]
17. Smyth DJ, et al. FUT2 nonsecretor status links type 1 diabetes susceptibility and resistance to infection. Diabetes. 2011; 60:3081–3084.10.2337/db11-0638 [PubMed: 22025780]
18. Imbert-Marcille BM, et al. A FUT2 gene common polymorphism determines resistance to rotavirus A of the P[8] genotype. J Infect Dis. 2014; 209:1227–1230.10.1093/infdis/jit655 [PubMed: 24277741]
19. Folseraas T, et al. Extended analysis of a genome-wide association study in primary sclerosing cholangitis detects multiple novel risk loci. J Hepatol. 2012; 57:366–375.10.1016/j.jhep.2012.03.031 [PubMed: 22521342]
20. Kashyap PC, et al. Genetically dictated change in host mucus carbohydrate landscape exerts a diet-dependent effect on the gut microbiota. Proc Natl Acad Sci USA. 2013; 110:17059–17064.10.1073/pnas.1306070110 [PubMed: 24062455]
21. Rausch P, et al. Colonic mucosa-associated microbiota is influenced by an interaction of Crohn disease and FUT2 (Secretor) genotype. Proc Natl Acad Sci USA. 2011; 108:19030–19035.10.1073/pnas.1106408108 [PubMed: 22068912]
22. Sartor RB. Microbial influences in inflammatory bowel diseases. Gastroenterology. 2008; 134:577–594.10.1053/j.gastro.2007.11.059 [PubMed: 18242222]
23. Koopman JP, Stadhouders AM, Kennis HM, De Boer H. The attachment of filamentous segmented micro-organisms to the distal ileum wall of the mouse: A scanning and transmission electron microscopy study. Lab Anim. 1987; 21:48–52.10.1258/002367787780740743 [PubMed: 3560864]
24. Suzuki K, et al. Aberrant expansion of segmented filamentous bacteria in IgA-deficient gut. Proc Natl Acad Sci USA. 2004; 101:1981–1986.10.1073/pnas.0307317101 [PubMed: 14766966]
25. Gaboriau-Routhiau V, et al. The key role of segmented filamentous bacteria in the coordinated maturation of gut helper T cell responses. Immunity. 2009; 31:677–689.10.1016/j.immuni.2009.08.020 [PubMed: 19833089]
26. Ivanov II, et al. Induction of intestinal Th17 cells by segmented filamentous bacteria. Cell. 2009; 139:485–498.10.1016/j.cell.2009.09.033 [PubMed: 19836068]
27. Ivanov II, et al. Specific microbiota direct the differentiation of IL-17-producing T-helper cells in the mucosa of the small intestine. Cell Host Microbe. 2008; 4:337–349.10.1016/j.chom.2008.09.009 [PubMed: 18854238]
28. Davis CP, Savage DC. Habitat, succession, attachment, and morphology of segmented, filamentous microbes indigenous to the murine gastrointestinal tract. Infect Immun. 1974; 10:948–956. [PubMed: 4426712]

29. Umesaki Y, Setoyama H, Matsumoto S, Imaoka A, Itoh K. Differential roles of segmented filamentous bacteria and clostridia in development of the intestinal immune system. Infect Immun. 1999; 67:3504–3511. [PubMed: 10377132]
30. Ivanov II, et al. The orphan nuclear receptor RORγt directs the differentiation program of proinflammatory IL-17$^+$ T helper cells. Cell. 2006; 126:1121–1133.10.1016/j.cell.2006.07.035 [PubMed: 16990136]
31. Spits H, et al. Innate lymphoid cells—A proposal for uniform nomenclature. Nat Rev Immunol. 2013; 13:145–149.10.1038/nri3365 [PubMed: 23348417]
32. Spits H, Di Santo JP. The expanding family of innate lymphoid cells: Regulators and effectors of immunity and tissue remodeling. Nat Immunol. 2011; 12:21–27.10.1038/ni.1962 [PubMed: 21113163]
33. Yokota Y, et al. Development of peripheral lymphoid organs and natural killer cells depends on the helix-loop-helix inhibitor Id2. Nature. 1999; 397:702–706.10.1038/17812 [PubMed: 10067894]
34. Eberl G, et al. An essential function for the nuclear receptor RORγ(t) in the generation of fetal lymphoid tissue inducer cells. Nat Immunol. 2004; 5:64–73.10.1038/ni1022 [PubMed: 14691482]
35. Sawa S, et al. RORγt$^+$ innate lymphoid cells regulate intestinal homeostasis by integrating negative signals from the symbiotic microbiota. Nat Immunol. 2011; 12:320–326.10.1038/ni.2002 [PubMed: 21336274]
36. Sonnenberg GF, Monticelli LA, Elloso MM, Fouser LA, Artis D. CD4(+) lymphoid tissue-inducer cells promote innate immunity in the gut. Immunity. 2011; 34:122–134.10.1016/j.immuni.2010.12.009 [PubMed: 21194981]
37. Buonocore S, et al. Innate lymphoid cells drive interleukin-23-dependent innate intestinal pathology. Nature. 2010; 464:1371–1375.10.1038/nature08949 [PubMed: 20393462]
38. Pickert G, et al. STAT3 links IL-22 signaling in intestinal epithelial cells to mucosal wound healing. J Exp Med. 2009; 206:1465–1472.10.1084/jem.20082683 [PubMed: 19564350]
39. Sonnenberg GF, Fouser LA, Artis D. Functional biology of the IL-22-IL-22R pathway in regulating immunity and inflammation at barrier surfaces. Adv Immunol. 2010; 107:1–29.10.1016/B978-0-12-381300-8.00001-0 [PubMed: 21034969]
40. Tsuji M, et al. Requirement for lymphoid tissue-inducer cells in isolated follicle formation and T cell-independent immunoglobulin A generation in the gut. Immunity. 2008; 29:261–271.10.1016/j.immuni.2008.05.014 [PubMed: 18656387]
41. De Togni P, et al. Abnormal development of peripheral lymphoid organs in mice deficient in lymphotoxin. Science. 1994; 264:703–707.10.1126/science.8171322 [PubMed: 8171322]
42. Chessa D, Winter MG, Jakomin M, Bäumler AJ. *Salmonella enterica* serotype Typhimurium Std fimbriae bind terminal α (1,2)fucose residues in the cecal mucosa. Mol Microbiol. 2009; 71:864–875.10.1111/j.1365-2958.2008.06566.x [PubMed: 19183274]
43. Awoniyi M, Miller SI, Wilson CB, Hajjar AM, Smith KD. Homeostatic regulation of *Salmonella*-induced mucosal inflammation and injury by IL-23. PLOS One. 2012; 7:e37311.10.1371/journal.pone.0037311 [PubMed: 22624013]
44. Godinez I, et al. T cells help to amplify inflammatory responses induced by *Salmonella enterica* serotype Typhimurium in the intestinal mucosa. Infect Immun. 2008; 76:2008–2017.10.1128/IAI.01691-07 [PubMed: 18347048]
45. Tumanov AV, et al. Lymphotoxin controls the IL-22 protection pathway in gut innate lymphoid cells during mucosal pathogen challenge. Cell Host Microbe. 2011; 10:44–53.10.1016/j.chom.2011.06.002 [PubMed: 21767811]
46. Domino SE, Zhang L, Gillespie PJ, Saunders TL, Lowe JB. Deficiency of reproductive tract α(1,2)fucosylated glycans and normal fertility in mice with targeted deletions of the FUT1 or FUT2 α(1,2)fucosyltransferase locus. Mol Cell Biol. 2001; 21:8336–8345.10.1128/MCB.21.24.8336-8345.2001 [PubMed: 11713270]
47. Kreymborg K, et al. IL-22 is expressed by Th17 cells in an IL-23-dependent fashion, but not required for the development of autoimmune encephalomyelitis. J Immunol. 2007; 179:8098–8104.10.4049/jimmunol.179.12.8098 [PubMed: 18056351]

48. Rakoff-Nahoum S, Paglino J, Eslami-Varzaneh F, Edberg S, Medzhitov R. Recognition of commensal microflora by toll-like receptors is required for intestinal homeostasis. Cell. 2004; 118:229–241.10.1016/j.cell.2004.07.002 [PubMed: 15260992]

49. Matsuki T, et al. Quantitative PCR with 16*S* rRNA-gene-targeted species-specific primers for analysis of human intestinal bifidobacteria. Appl Environ Microbiol. 2004; 70:167–173.10.1128/AEM.70.1.167-173.2004 [PubMed: 14711639]

50. Kibe R, Sakamoto M, Hayashi H, Yokota H, Benno Y. Maturation of the murine cecal microbiota as revealed by terminal restriction fragment length polymorphism and 16*S* rRNA gene clone libraries. FEMS Microbiol Lett. 2004; 235:139–146.10.1111/j.1574-6968.2004.tb09578.x [PubMed: 15158273]

51. Jang MH, et al. Intestinal villous M cells: An antigen entry site in the mucosal epithelium. Proc Natl Acad Sci USA. 2004; 101:6110–6115.10.1073/pnas.0400969101 [PubMed: 15071180]

52. Obata T, et al. Indigenous opportunistic bacteria inhabit mammalian gut-associated lymphoid tissues and share a mucosal antibody-mediated symbiosis. Proc Natl Acad Sci USA. 2010; 107:7419–7424.10.1073/pnas.1001061107 [PubMed: 20360558]

53. Yamamoto M, Fujihashi K, Kawabata K, McGhee JR, Kiyono H. A mucosal intranet: Intestinal epithelial cells down-regulate intraepithelial, but not peripheral, T lymphocytes. J Immunol. 1998; 160:2188–2196. [PubMed: 9498757]

54. Ohta N, et al. IL-15-dependent activation-induced cell death-resistant Th1 type CD8 α β^{+}NK1.1^{+} T cells for the development of small intestinal inflammation. J Immunol. 2002; 169:460–468.10.4049/jimmunol.169.1.460 [PubMed: 12077277]

55. Yoshida H, et al. IL-7 receptor α^{+} CD3(–) cells in the embryonic intestine induces the organizing center of Peyer's patches. Int Immunol. 1999; 11:643–655.10.1093/intimm/11.5.643 [PubMed: 10330270]

56. Yamamoto M, et al. Role of gut-associated lymphoreticular tissues in antigen-specific intestinal IgA immunity. J Immunol. 2004; 173:762–769.10.4049/jimmunol.173.2.762 [PubMed: 15240662]

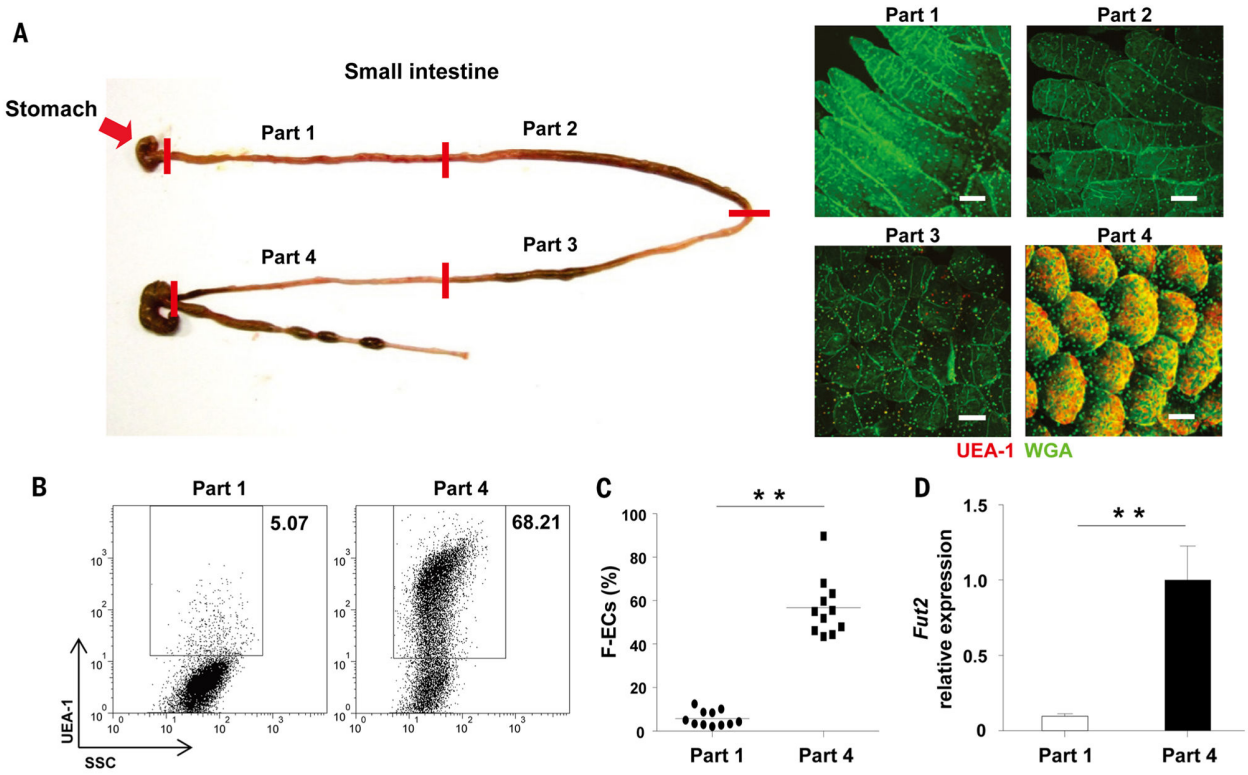

Fig. 1. F-ECs are dominant in the ileum

(**A**) Mouse small intestines were divided equally into 4 parts (parts 1, 2, 3, and 4), from the proximal (duodenum) to the distal (ileum) ends (left), and whole-mount tissues were stained with UEA-1 (red) and WGA (green) to detect F-ECs (UEA-1$^+$ WGA$^+$ cells) (right). Scale bars, 100 μm. Data are representative of three independent experiments. (**B** and **C**) Flow cytometric analysis of intestinal ECs isolated from part 1 and part 4 of the small intestines of C57BL/6 (B6) mice. Representative dot-plots are shown in (B). Percentages and mean numbers (horizontal bars) of fucosylated epithelial cells (n = 11 mice per group) are shown (C). SSC, side scatter. Data of two independent experiments are combined. (**D**) Expression of *Fut2* in ECs isolated from part 1 and part 4 of the small intestine isolated from five to six mice per group. Error bars indicate SD. $^{**}P < 0.01$ by using Student's t test. Data are representative of two independent experiments.

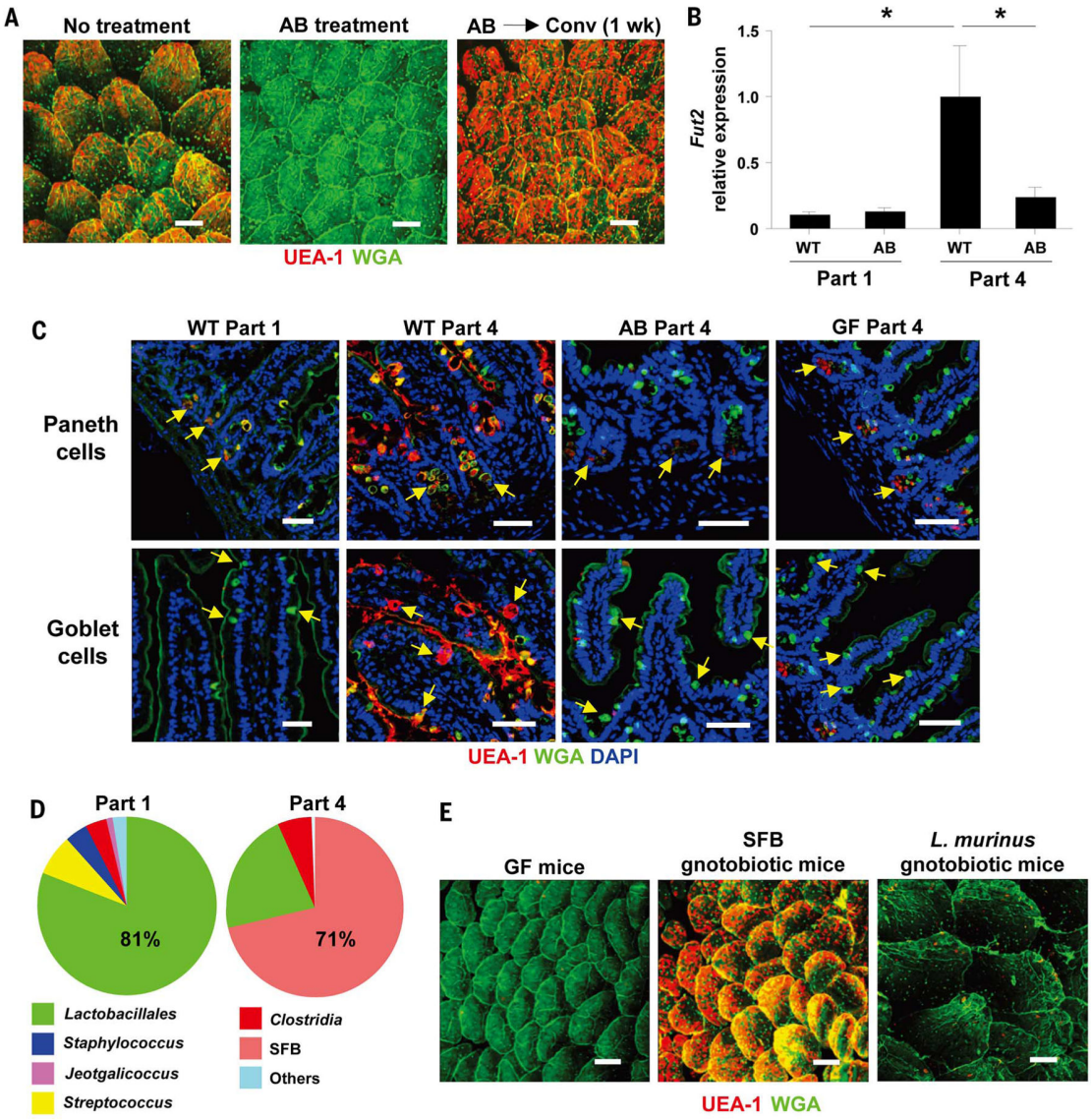

Fig. 2. Commensal bacteria induce epithelial fucosylation under homeostatic conditions

(**A**) Whole-mount ileal tissues of AB-treated mice and conventionalized AB-treated mice were stained with UEA-1 (red) and WGA (green) (n = 3 mice per group). Scale bars, 100 μm. Data are representative of two independent experiments. (**B**) *Fut2* expression in ECs isolated from part 1 (duodenum) and part 4 (ileum) of the small intestines of wild-type (WT) and AB-treated mice (n = 3 mice per group). Error bars indicate SD. *$P < 0.05$ by using Student's t test. Data are representative of two independent experiments. (**C**) Tissues from part 1 and part 4 of the small intestines of WT, AB-treated, and GF mice were stained with UEA-1 (red), WGA (green), and 4′,6-diamidino-2-phenylindole (DAPI) (blue). Arrows show Paneth cells (top) and goblet cells (bottom). Scale bars, 50 μm. Data are representative of two independent experiments. (**D**) Bacterial populations isolated from the mucus fraction of part 1 and part 4 of mouse small intestine were analyzed by means of 16*S* rRNA gene clone library. Representative graphs were constructed from samples (part 1, n = 480 clones;

Part 4, $n = 477$ clones) isolated from five different mice (95 or 96 samples were obtained from each mouse). (**E**) Ileal tissues of GF, SFB, or *L. murinus* mono-associated mice ($n = 3$ mice per group) were stained with UEA-1 (red) and WGA (green). Scale bars, 100 μm. Data are representative of two independent experiments.

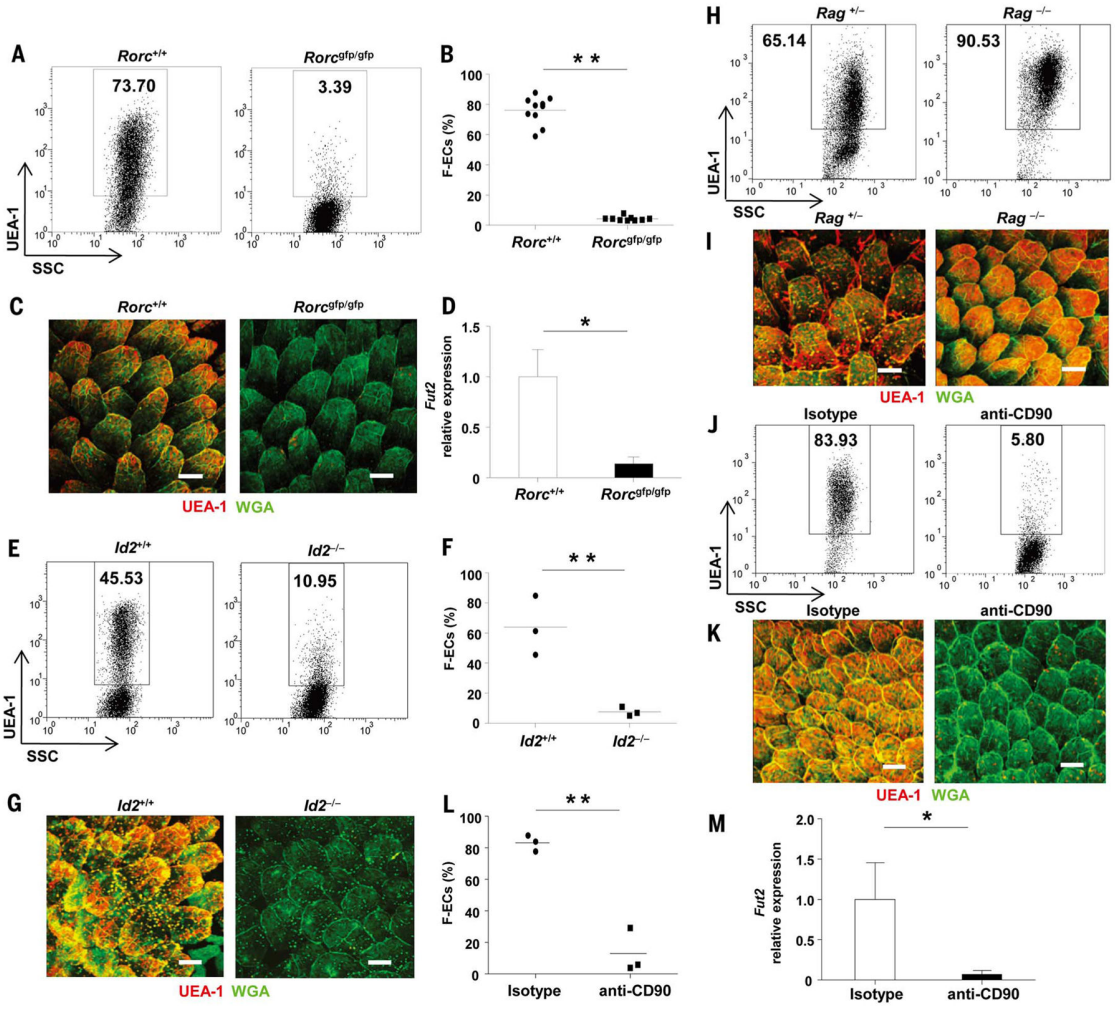

Fig. 3. CD90$^+$ RORγt$^+$ ILC3 induce F-ECs

(**A** and **B**) Representative dot-plots (A) and percentages and means (B) (horizontal bars) of ileal F-ECs isolated from *Rorc*$^{+/+}$ and *Rorc*$^{gfp/gfp}$ mice (n = 10 mice per group). SSC, side scatter. $^{**}P < 0.01$ by using Student's t test. Data of two independent experiments are combined. (**C**) Whole-mount ileal tissues from *Rorc*$^{+/+}$ and *Rorc*$^{gfp/gfp}$ mice were stained with UEA-1 (red) and WGA (green) (n = 10 mice per group). Scale bars, 100 μm. Data are representative of two independent experiments. (**D**) Expression of *Fut2* in ileal ECs isolated from *Rorc*$^{+/+}$ and *Rorc*$^{gfp/gfp}$ mice (n = 5 mice per group). Data are representative of two independent experiments. Error bars indicate SD. $^{*}P < 0.05$. (**E** and **F**) Representative dot-plots (E) and percentages and means (F) (horizontal bars) of ileal ECs isolated from *Id2*$^{+/+}$ and *Id2*$^{-/-}$ mice (n = 3 mice per group). Data of three independent experiments are combined. (**G**) Whole-mount staining of ileal villi isolated from *Id2*$^{+/+}$ and *Id2*$^{-/-}$ mice. Scale bars, 100 μm. Data are representative of three independent experiments. (**H** and **J**) Representative dot-plots of ileal ECs isolated from *Rag*$^{+/-}$ and *Rag*$^{-/-}$ mice (H) and *Rag*$^{-/-}$ mice treated with mAb to CD90 (anti-CD90 mAb) or isotype control Ab to CD90 (J) (n = 3 mice per group). (**I** and **K**) Whole-mount staining of ileal villi isolated from *Rag*$^{+/-}$ or

Rag$^{-/-}$ mice (I) and anti-CD90 mAb– or anti-CD90 isotype control Ab–treated *Rag*$^{-/-}$ mice (K) ($n = 3$ mice per group). Scale bars, 100 μm. Data are representative of two independent experiments. (**L** and **M**) Percentages and means (horizontal bars) of ileal F-ECs (L) and *Fut2* expression (M) isolated from anti-CD90 mAb– or isotype control Ab–treated *Rag*$^{-/-}$ mice ($n = 3$ mice per group). Data are representative of two independent experiments. Error bars indicate SD. *$P < 0.05$, **$P < 0.01$ by using Student's *t* test.

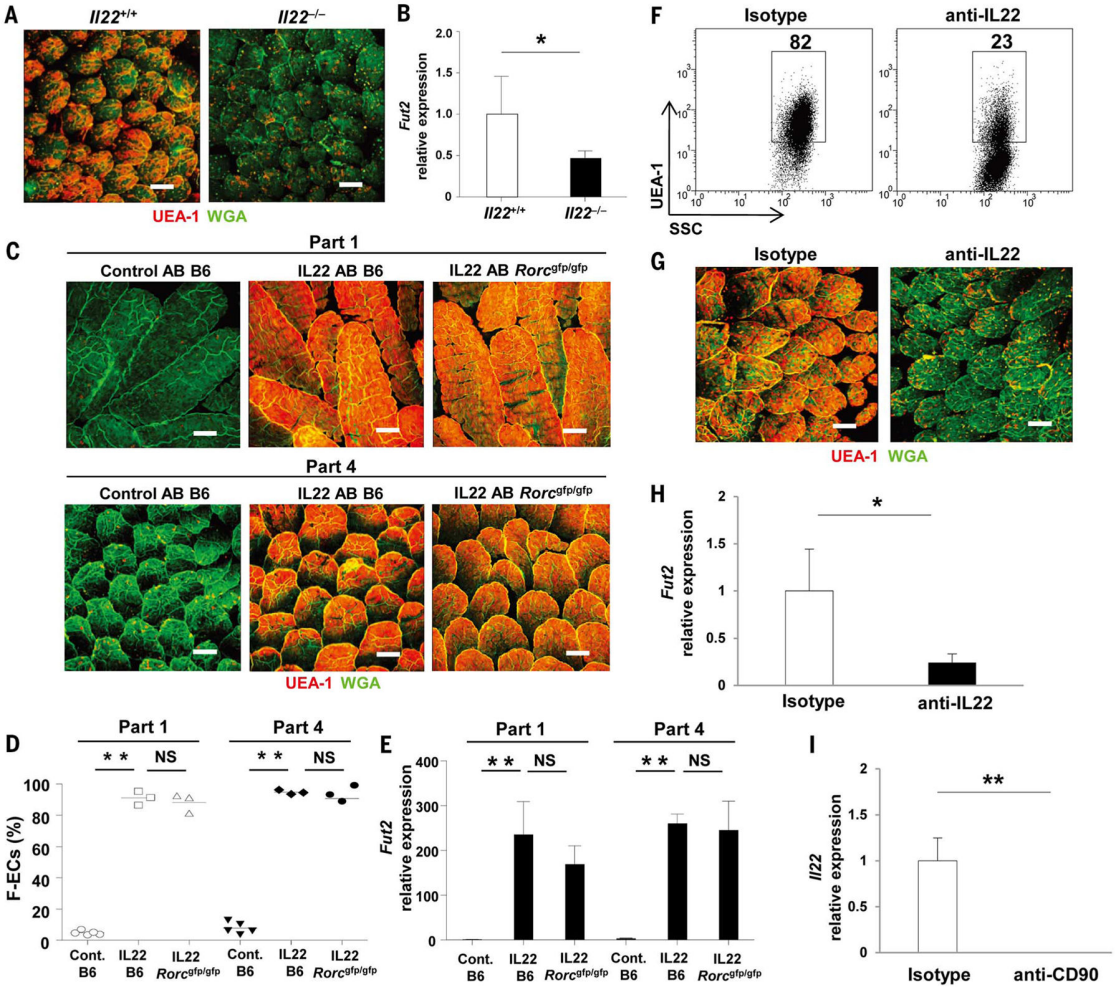

Fig. 4. IL-22 produced by ILCs is involved in the induction of F-ECs

(**A** and **B**) Whole-mount tissues stained with UEA-1 (red) and WGA (green) (A) and gene expression of *Fut2* (B) in ileal villi isolated from $Il22^{+/+}$ or $Il22^{-/-}$mice ($n = 6$ mice per group). Error bars indicate SD. $^{*}P < 0.05$ by using Student's *t* test. Scale bars, 100 μm. Data are representative of two independent experiments. (**C** to **E**) AB-treated C57BL/6 (B6) or $Rorc^{gfp/gfp}$ mice were intravenously injected with IL-22–encoding plasmid or control vector. Whole-mount staining (C), frequency of F-ECs (D) (mean, horizontal bars), and Fut2 mRNA expression was analyzed by means of rRT-PCR ($n \geq 3$ mice per group) (E). Scale bars, 100 μm. Error bars indicate SD. $^{**}P < 0.01$ by using Student's *t* test. NS, not significant. Data are representative of two independent experiments. (**F** to **H**) Representative dot-plots (F), whole-mount histological images (G), and expression of *Fut2* (H) of ileal ECs isolated from $Rag^{-/-}$ mice treated with antibody to IL-22 or control Ab. Scale bars, 100 μm. Error bars indicate SD. $^{*}P < 0.05$ by using Student's *t* test. (**I**) Expression of *Il22* in ileal LP cells from $Rag^{-/-}$ mice treated with antibody to CD90 or control Ab. Error bars inidicate SD. $^{**}P < 0.01$ by using Student's *t* test. Data are representative of two independent experiments.

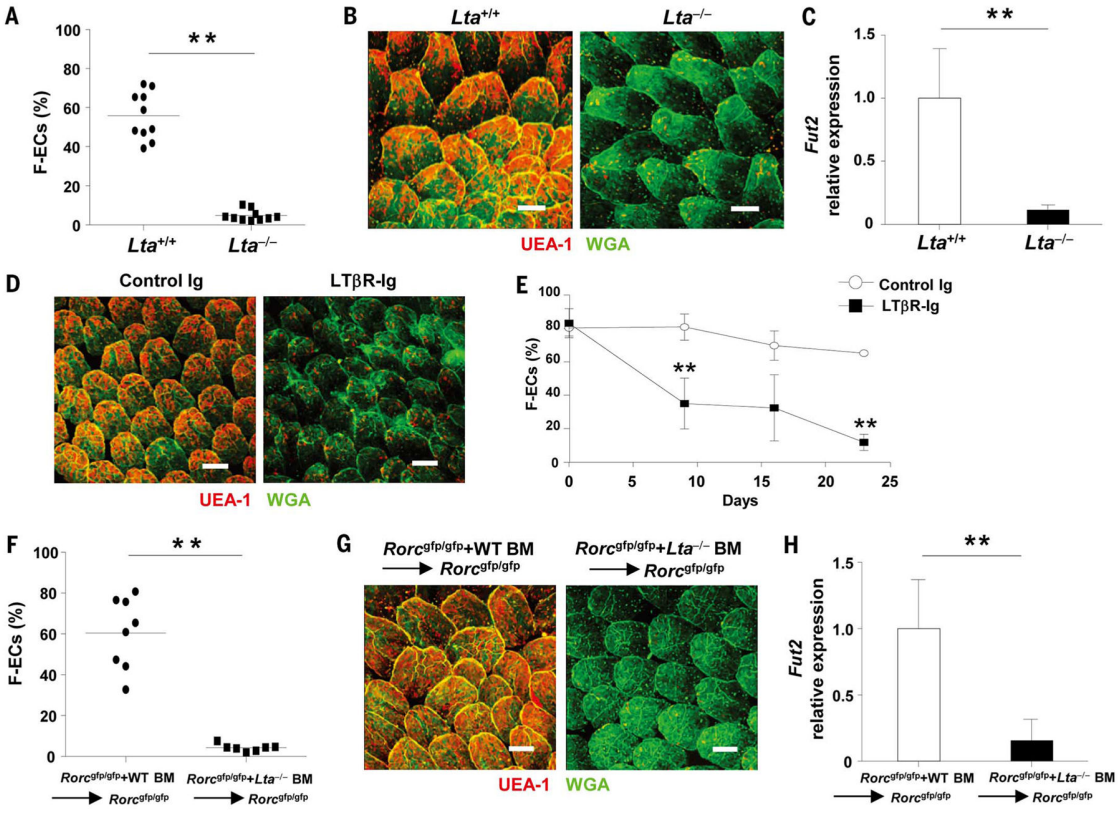

Fig. 5. LTs in innate lymphoid cells induce F-ECs

(**A**) Representative values and means (horizontal bars) of frequency of ileal F-ECs isolated from *Lta*$^{+/+}$ or *Lta*$^{-/-}$ mice (n = 10 mice per group). Data of two independent experiments are combined. $^{**}P < 0.01$ by using Student's t test. (**B**) Representative whole-mount staining of ileal villi isolated from *Lta*$^{+/+}$ or *Lta*$^{-/-}$ mice (n = 10 mice per group). Scale bars, 100 μm. (**C**) Expression of *Fut2* in ileal ECs isolated from *Lta*$^{+/+}$ or *Lta*$^{-/-}$ mice (n = 5 mice per group). Error bars inidicate SD. $^{**}P < 0.01$ by using Student's t test. Data are representative of two independent experiments. (**D**) Representative whole-mount staining of ileal villi from C57BL/6 mice injected with control IgG or LTβR-Ig. Tissues were stained with UEA-1 (red) and WGA (green). (n = 3 mice per group) (**E**) Frequencies of F-ECs in the ileum of C57BL/6 mice injected with control IgG (control Ab) or LTβR-Ig twice (day 9), 3 times (day 16), or 4 times (day 23) (n = 3 mice per group). Error bars indicate SD. $^{**}P <$ 0.01 by using Student's t test. (**F** to **H**) Values and means (F), representative whole-mount staining (G), and expression of *Fut2* (H) in ileal ECs isolated from *Rorc*$^{gfp/gfp}$ mice injected with a mixture of BM cells from *Rorc*$^{gfp/gfp}$ and WT mice or *Rorc*$^{gfp/gfp}$ and *Lta*$^{-/-}$ mice (n = 7 to 8 mice per group). Data of two independent experiments are combined. Error bars indicate SD. $^{**}P < 0.01$ by using Student's t test. Scale bars, 100 μm.

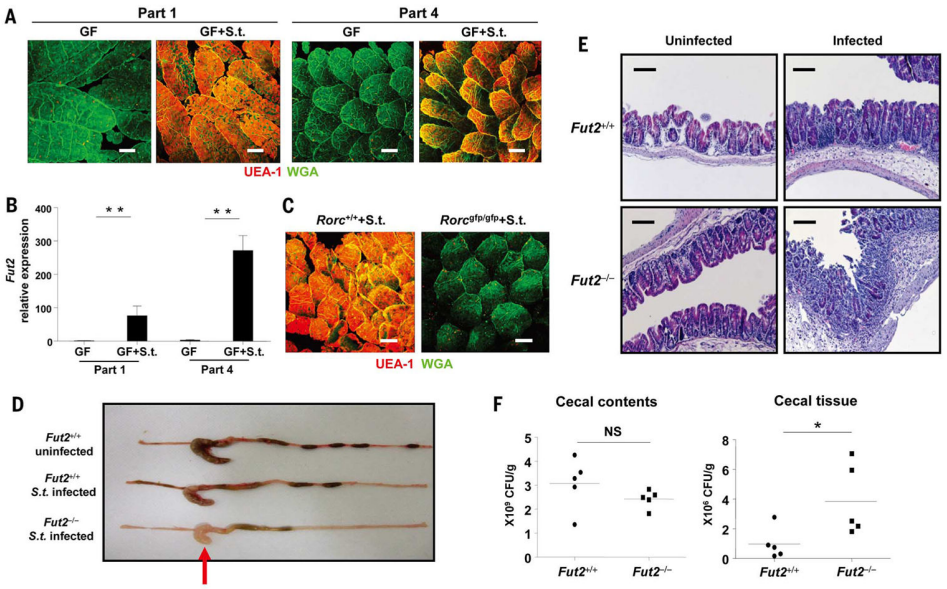

Fig. 6. Epithelial fucosylation protects against infection by *S. typhimurium*

(**A**) Whole-mount tissues from part 1 (duodenum) and part 4 (ileum) of the small intestines of germ-free (GF) or *S. typhimurium*–infected GF mice were stained with UEA-1 (red) and WGA (green) ($n = 3$ to 4 mice per group). Scale bars, 100 μm. (**B**) Epithelial Fut2 expression in part 1 and part 4 of the small intestines of GF and *S. typhimurium*–infected GF mice was analyzed by using quantitative PCR ($n = 3$ to 4 mice per group). Error bars indicate SD. $^{**}P < 0.01$ by using Student's *t* test. (**C**) Whole-mount tissues from ileum of *S. typhimurium*–infected $Rorc^{+/+}$ or $Rorc^{gfp/gfp}$ mice were isolated and stained with UEA-1 (red) and WGA (green) ($n = 3$ to 4 mice per group). Scale bars, 100 μm. (**D** and **E**) $Fut2^{+/+}$ or $Fut2^{-/-}$ mice were infected with *S. typhimurium*. Red arrow shows inflammation of the cecum. Representative macroscopic images (D) and hematoxylin and eosin–stained cecal sections (E) of infected or uninfected mice ($n = 5$ mice per group). Scale bars, 100 μm. (**F**) Numbers of bacteria in the luminal contents, and within the tissues, of the ceca of $Fut2^{+/+}$ or $Fut2^{-/-}$ mice were counted 24 hours after infection ($n = 5$ mice per group). $^{*}P < 0.05$ by using Student's *t* test. NS, not significant. Three independent experiments were performed with similar results.

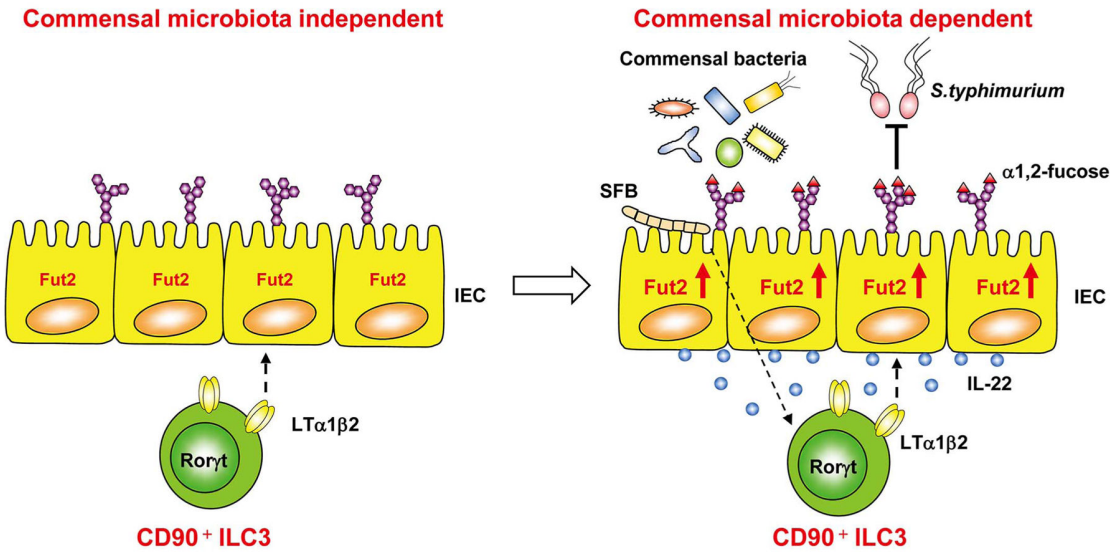

Fig. 7. Scheme for the induction and regulation of epithelial fucosylation by ILC3

IL-22– and LTα-producing ILC3 are critical cells for the induction and regulation of F-ECs. ILC3-mediated fucosylation of ECs is operated by commensal microbiota–dependent and –independent manners. Commensal bacteria, including SFB, stimulate CD90$^+$ ILC3 to produce IL-22 for the induction of Fut2 in ECs. On the other hand, LTα production by ILC3 are operated by a commensal bacteria–independent manner. ILC3-derived IL-22 and LTα induce Fut2 and subsequent epithelial fucosylation, which inhibits infection by *S. typhimurium*. IEC, intestinal epithelial cell.